EUREKA CHANNEL BRIDGE: SEISMIC RESPONSE AND SYSTEM IDENTIFICATION

Ahmed Elgamal[1], Ning Wang[2], and John Li[1]

[1] University of California, San Diego, Dept. of Structural Engineering, La Jolla, CA 92093-0085
[2] Institute of Geophysics, China Earthquake Administration, Beijing, 100081, China

Abstract

A unique opportunity for gaining insights is facilitated by availability of the CSMIP Eureka Channel Bridge seismic records. Of special interest is the recorded response of a bridge pier at the deck, pile cap and within the underlying pile foundation. In this study, recorded response from the strongest to date 2010 Ferndale earthquake (PGA of about 0.25g), along with other available low-amplitude events are employed to evaluate the pile foundation, and overall bridge seismic response. Finite Element modeling is employed along with the optimization framework SNOPT, to derive salient characteristics of the overall bridge system response.

Introduction

A large set of earthquake records from the highly instrumented Eureka Channel bridge-ground system (Figure 1) has been compiled and made available by the California Geological Survey (http://www.strongmotioncenter.org). During a large number of seismic events, more than 20 data channels have been documenting the seismic response of the deck, foundation, abutments, and adjacent ground surface. Of special interest is the response of a pier instrumented at the deck, pile cap, and below ground in the foundation.

Bridge Configuration and Instrumentation

The Eureka Channel bridge configuration is shown in Figure 2. In this Figure, dense instrumentation is seen along the deck, at the abutments, and on the nearby ground surface. In addition, a Pier (E7) is instrumented at the pile cap and within the underlying pile foundation. It may be noted (Figure 2) that the bridge includes a substantial horizontal curve, which results in significant coupling in its longitudinal (LONG) and transverse (TRAN) response.

Significant variability in the ground stratification and soil properties may be observed (Figures 2). The soil profile (Figure 2) reveals that the site is mantled by very soft silty clay underlain by medium clay and compact gray sand. Stiff clay was encountered at the elevation of about -12 m and continues to the maximum explored depth. Soil layers vary in thickness and are not continuous horizontally (Caltrans 2002).

Earthquake Motions

Records from a large number of earthquakes (Table 1) during the period of June 2007 through March 2014 are currently available with Magnitudes in the range of 4.5 M_L (local magnitude) to 6.8 M_w (moment magnitude). To date, the highest levels of recorded acceleration are due to the 2010 $M_w = 6.5$ Ferndale Earthquake approximately 35 km away from Ferndale, CA in a deformation zone of the southernmost Gorda Plate (http://earthquake.usgs.gov, Storesund et al. 2010). During this event, the recorded Transverse peak acceleration was 0.25 g at the ground surface near the bridge, and 0.51 g at the bridge deck.

(a)

(b)

Figure 1. Bridge Configuration: (a) Samoa Channel Bridge, Eureka Geotechnical Array, Middle Channel Bridge and Eureka Channel Bridge (Map Data @ 2015 Google), and (b) Close-up of the Eureka Channel Bridge (http://www.strongmotioncenter.org)

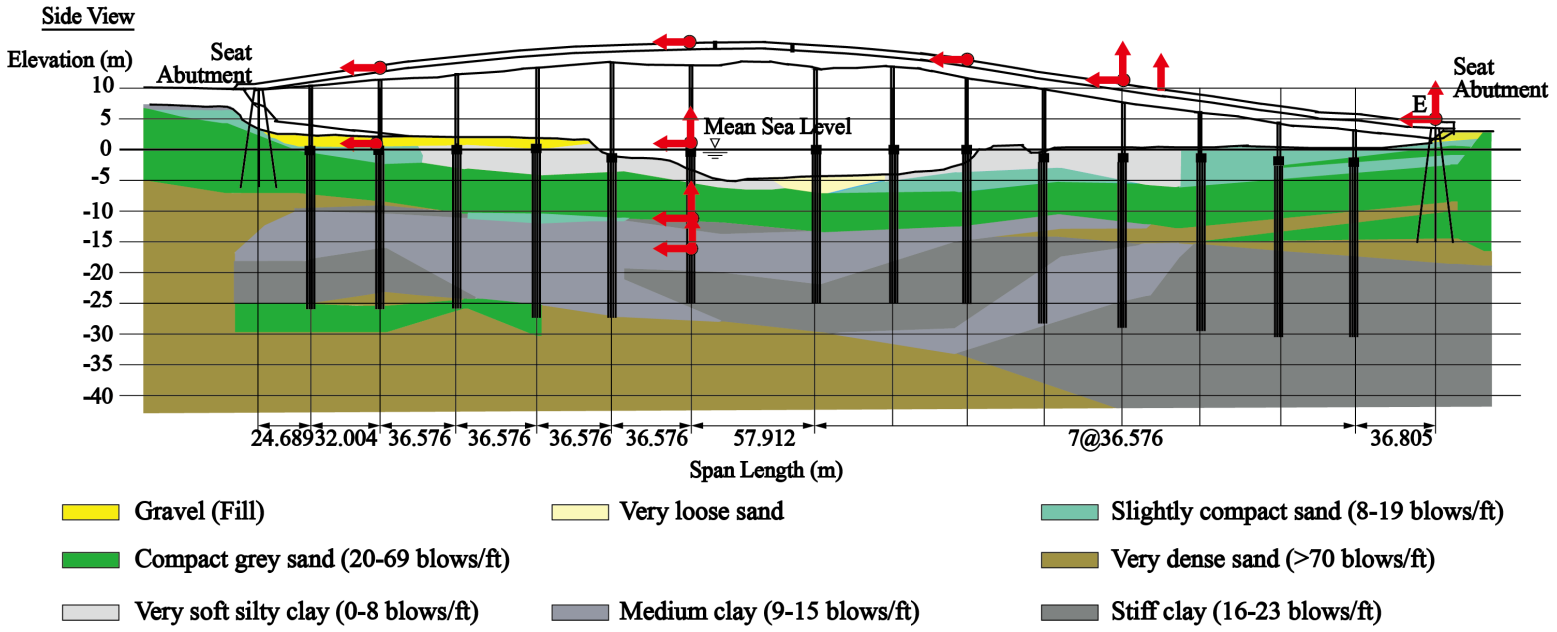

(a)

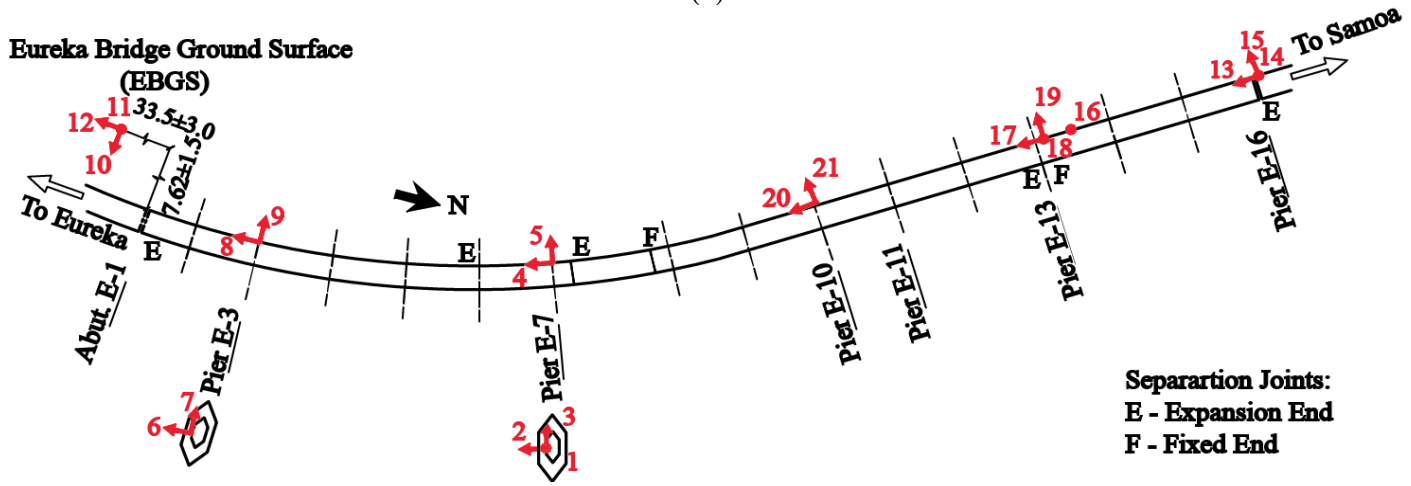

(b)

Figure 2. Layout of Instrumentation at the Eureka Channel Bridge: (a) Bridge-ground side view (Caltrans 2002), and (b) Plan view (http://www.strongmotioncenter.org)

Table 1 Recorded earthquakes at the bridge site (arranged by order of peak acceleration)

Earthquake	Epicentral Distance (km)	Horizontal Peak Acceleration (g)			
		E-7 Pile -16.46 m		**Bridge**	
		TRAN	LONG	TRAN	LONG
Ferndale 2010* (M_w=6.5)	54.5	0.130	0.158	0.510	0.955** 0.540***
Ferndale 2014 (M_w=6.8)	82.7	0.020	0.014	0.072	0.048
Trinidad 2008 (M_w=4.6)	41.7	0.009	0.013	0.060	0.047
Humboldt Hill 2013 (M_L=4.5)	20.8	0.009	0.008	0.019	0.014
Trinidad 2007 (M_L=5.1)	65.6	0.018	0.007	0.081	0.031
Ferndale 2010 Feb (M_w=5.9)	77.8	0.013	0.009	0.046	0.022
Willow Creek 2008 (M_w=5.4)	55.4	0.007	0.004	0.026	0.017
Ferndale 2007 (M_L=5.4)	63.3	0.005	0.006	0.021	0.014

*The January 2010 Ferndale Earthquake will be referred to as "the moderate event" in this study
**Large peak acceleration due to spikes from separation joints (Huang and Shakal 1995; Malhotra et al. 1995)
***Estimated after removing spikes using a band-pass filter

Eureka Channel Bridge and Pier E7

In this section representative responses of the bridge are presented. Figure 3 displays the bridge relative displacement referenced to the -16.46 m pile motion (essentially the ground motion at this depth) for the 2007 Ferndale event. All along the deck, predominant in-phase response is noted in both directions (TRAN defined as radially inward for this curved bridge). The bridge is seen to be noticeably more flexible in the mid-span zone (e.g. Channels 4 and 5 at Pier E-7), with the relatively tall compliant pier at this location (Figure 2).

Transverse displacement along Pier E-7 at the four instrumented elevations (Figure 2) is shown in Figure 4. In-phase response with a dominant fundamental period is evident (about 0.65 seconds). Furthermore, it can be seen (Figure 4) that the pile cap as well as the bridge deck displacements display a significant level of amplification. In general, the pier deformation is evenly accounted for by the column and the pile group deformations in both the transverse and longitudinal directions.

Pier E-7 Seismic Response

In an effort to gain preliminary insights, the transverse recorded seismic motion of Pier E-7 was studied, based on its tributary section of the bridge deck (Wang 2015). This idealization in the transverse direction is partially substantiated by presence of separation joints at the adjacent bents (Figure 2).

Utilizing the recorded motions, the dynamic transverse response is investigated to identify lateral stiffness of the E-7 column and the foundation at this location. A sub-structuring

approach (Elgamal et al. 1996) is adopted where motion at any given depth is taken to define the "input" for the overlying structural domain.

As such, using a beam-column pier E-7 Finite Element (FE) idealization from the deck, down to the pile cap (Figure 2), column flexural rigidity was identified $(EI)_{id}$ by minimizing the difference between the computed and recorded Channel 5 deck response with the aid of SNOPT (Appendix A) to estimate a secant flexural rigidity. For that purpose, the recorded pile cap motion (Chan 3) at the base of the column is employed as the input base excitation. On this basis (Wang et al. 2020), it was found that the identified flexural rigidity $(EI)_{id}$ of the column (Table 3) was about 0.6 *EI* for low amplitude earthquake events (where *EI* is the un-cracked section bending stiffness). This estimate compares well with practical guidelines (e.g., Caltrans 2013). During the moderate shaking event, $(EI)_{id}$ instantaneous values reached as low as about 0.25 *EI,* with no signs of permanent reduction as the drift ratio diminished towards the end of shaking.

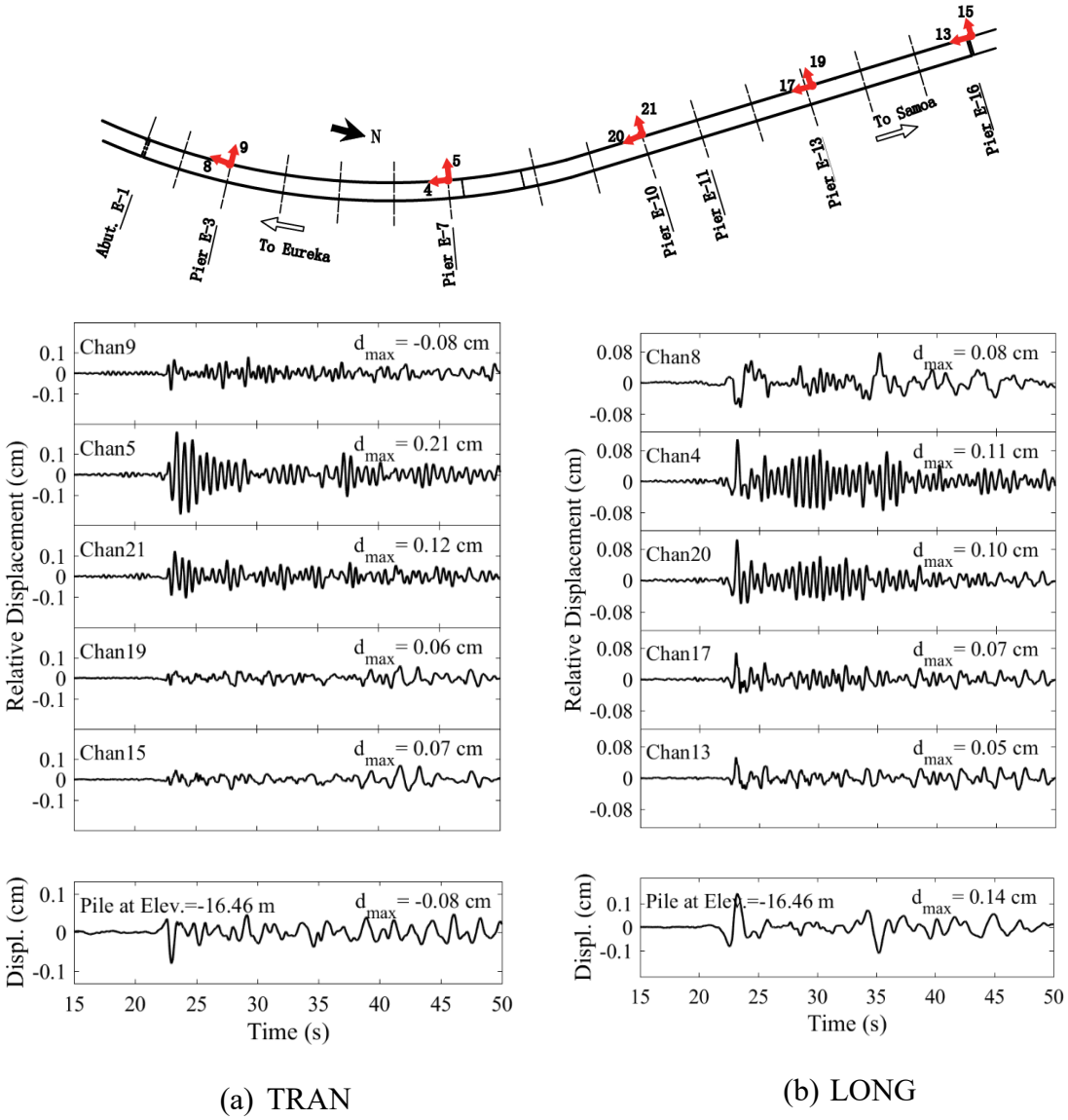

(a) TRAN (b) LONG

Figure 3. Relative displacement along the bridge deck during the 2007 Ferndale Earthquake

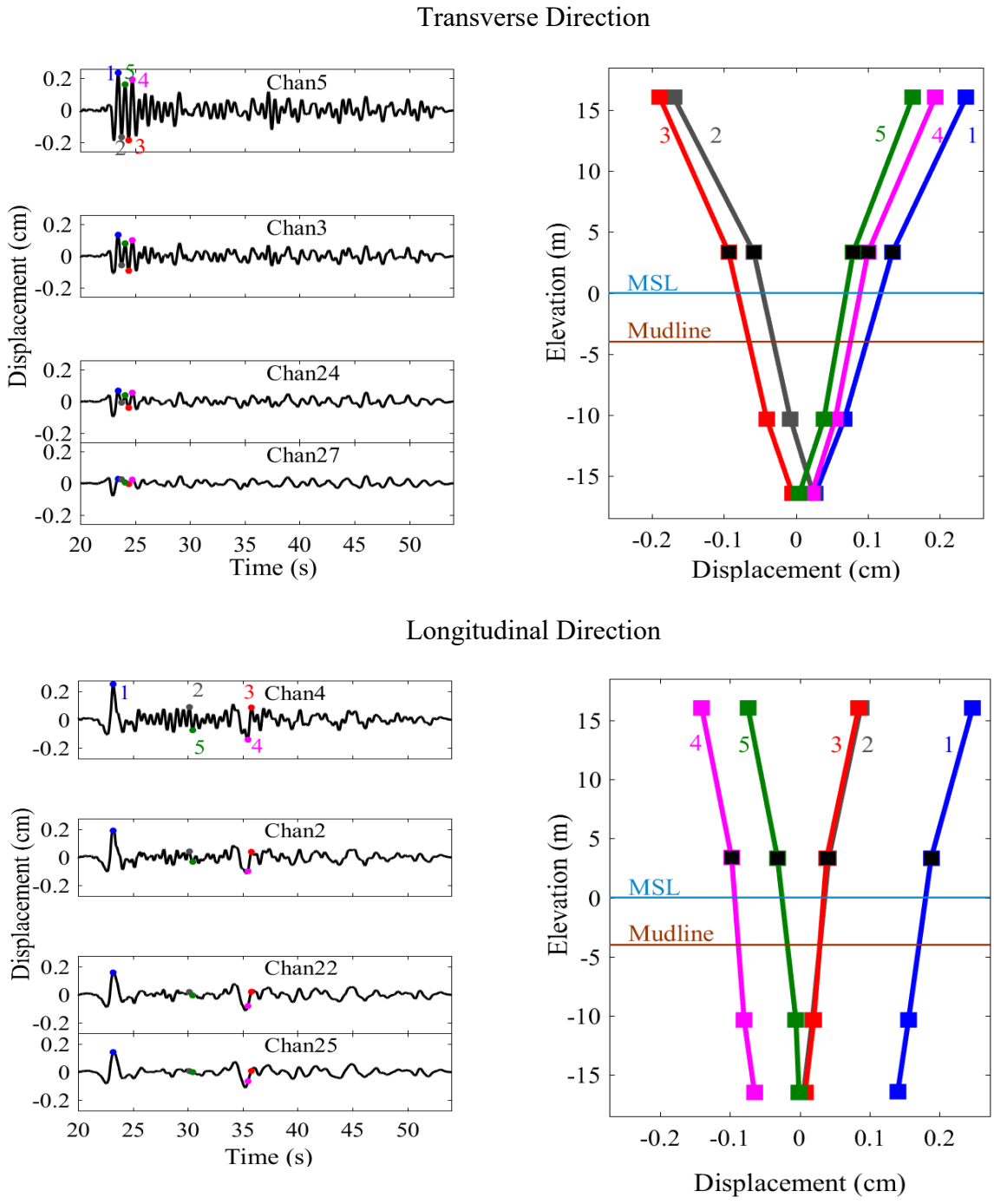

Figure 4. Time history of displacement and displaced configuration of Pier E7 at selected time instants during the 2007 Ferndale Earthquake

Using a similar approach, the estimated E-7 foundation stiffness clearly reflected the constraining effect of the soil surrounding the pile foundation. During the moderate event (Wang et al. 2020), instantaneous reductions in stiffness of about 50% were noted during the strongest phase of this shaking event.

Eureka Channel Bridge Lateral Foundation Stiffness

A beam-column model (202 elements) representing the entire Eureka Channel Bridge with its different column heights was developed (Wang et al. 2020). The graphical user interface MSBridge (Elgamal et al. 2014) was employed to generate the mesh for this curved bridge.

Focus was placed on the transverse response. Lateral springs were included at the base of the pier columns to account for stiffness of the underlying pile foundations and the associated soil-foundation-structure interaction (Lam and Martin 1986; Zafir 2002). These springs represent stiffness of the foundation down to an assumed uniform-excitation depth as defined by the recorded motion at -16.46 m. Using SNOPT (Appendix A), stiffness of the lateral springs was optimized so that the computed response is compatible with the recorded motions along the bridge super-structure (Wang et al. 2020). The results shown in Figure 5 suggest (compared to the Samoa Channel bridge scenario as reported in Wang et al. 2018):

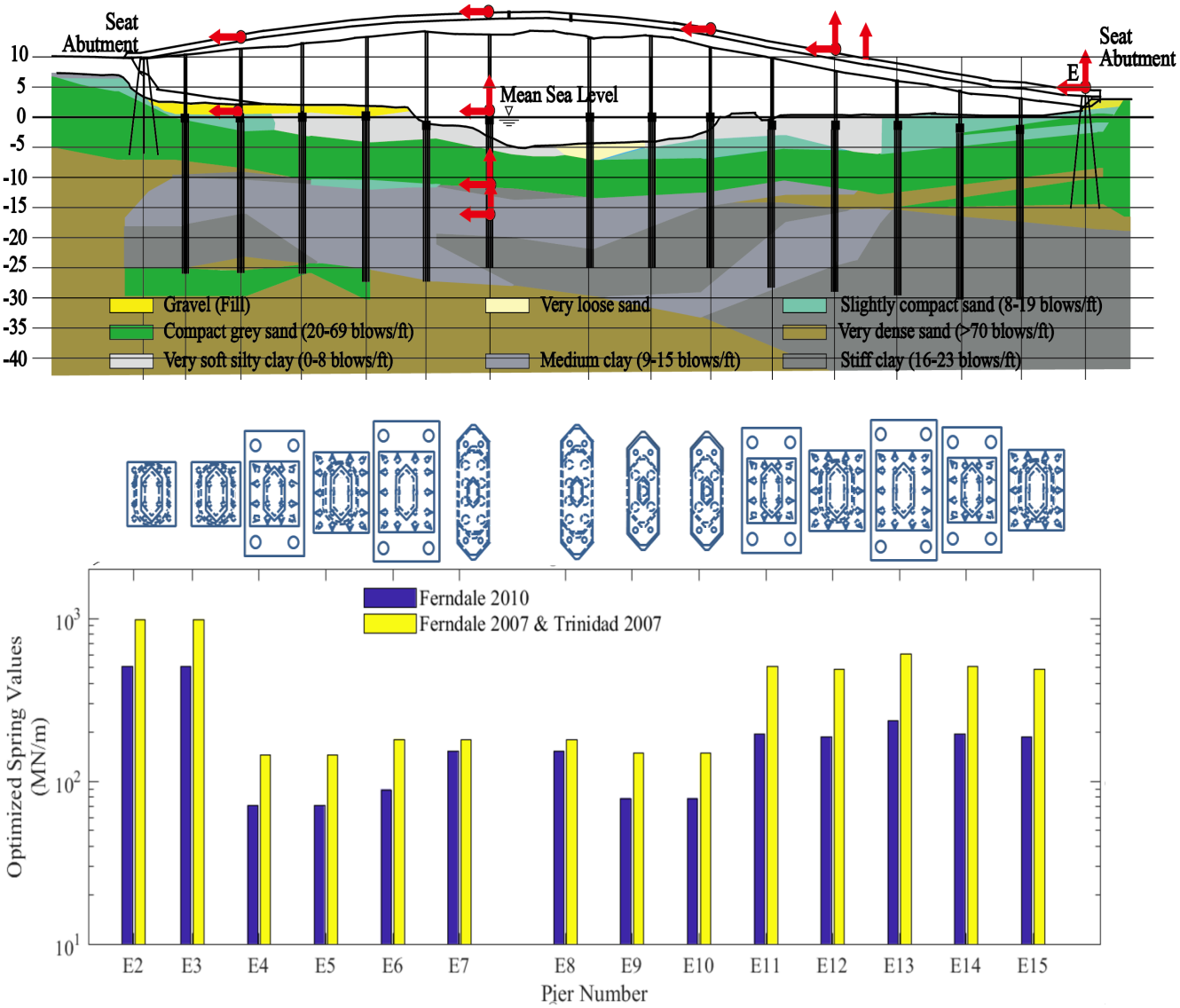

Figure 5. Identified Transverse direction base spring values along the Eureka Channel bridge

i) Foundation stiffness overall is higher,
ii) Reduction in stiffness during the strong shaking phase is pronounced, but to a lesser degree.
iii) Variability in stiffness along the bridge length is less pronounced.

Summary and Conclusions

The Eureka CSMIP seismic records (3 bridges and downhole array) constitute a unique invaluable resource for documentation of bridge and foundation response over a wide range of ground shaking scenarios. Inferred lateral stiffness of the involved pile-groups provides new insights about the actual foundation resistance at low and moderate levels of seismic excitation. These insights increase our confidence in current design/modeling assumptions, and allow for better understandings as relates to bridge response during strong earthquakes.

Acknowledgements

The research presented in this paper was funded by CSMIP, and partially by the China Earthquake Administration Grant (No. DQJB15B12). This support is gratefully acknowledged.

Appendix A

SNOPT (Sparse Nonlinear Optimization), a general-purpose numerical optimization code (Gill et al. 2002) was employed (Wang et al. 2020) to minimize the difference (Figure 6) between computed and recorded seismic response (Elgamal et al. 2004). The extended OpenSees-SNOPT framework, has been conveniently set up to perform this task (Gu 2008). For each earthquake simulation, OpenSees starts with a user-defined set of modeling parameters (initial guess), and an objective function Φ (measure of error) is computed using the recorded and computed responses. From there, SNOPT systematically conducts numerous OpenSees runs in which values of the modelling parameters are changed incrementally (re-computing Φ every time). Conceptually, if a lower Φ is found, values of the parameters are updated and the process continues until a minimum Φ is attained (thus defining optimal values of the numerical model parameters, Figure 6). A major advantage of SNOPT is that it requires relatively few evaluations of the objective function which helps speed up the time-consuming OpenSees simulations (Gu 2008).

The objective function was defined to be the sum of squared differences of computed and recorded seismic response at the sensor locations of interest (over any user-specified time interval):

$$\Phi = \sum_{i=1}^{Number\ of\ Sensors} \sum_{n=Start\ time\ step}^{End\ time\ step} (u_i(t_n) - u_i^{Rec}(t_n))^2$$

in which u is the OpenSees computed response (displacement or acceleration), u^{Rec} is the recorded instrumentation response, and t is time step (Wang et al. 2020).

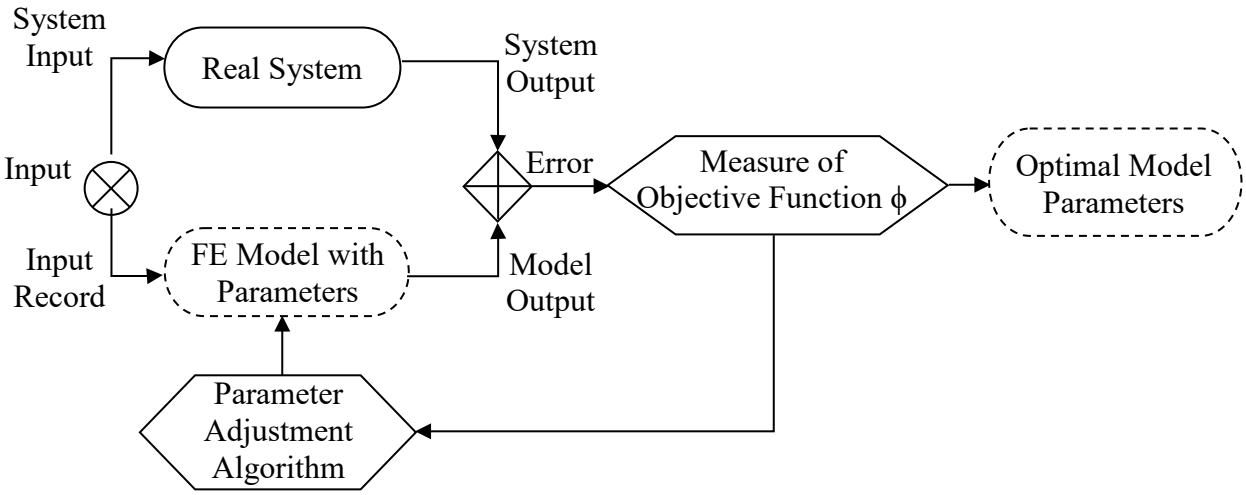

Figure 6. Block diagram illustrating the optimization procedure framework (after Zeghal 1990, Elgamal et al. 2004)

References

Caltrans (2002). "As-Built Plans, Earthquake Retrofit Project for Eureka Channel Bridge." California Department of Transportation, Sacramento, CA, [personal communication].

Caltrans (2013). "Seismic Design Criteria Version 1.7." California Department of Transportation, Sacramento, CA.

Elgamal, AW, Zeghal, M, Parra, E, Gunturi, R, Tang, HT, and Stepp, JC (1996). Identification and modeling of earthquake ground response - I. Site amplification. Soil Dynamics and Earthquake Engineering;15(8):499-522.

Elgamal A, Lai T, Gunturi R, Zeghal M. (2004). System identification of landfill seismic response. Journal of earthquake engineering;8(04):545-566.

Elgamal, A., Lu, J., and Mackie, K. (2014). "MSBridge: OpenSees Pushover and Earthquake Analysis of Multi-span Bridges - User Manual." Department of Structural Engineering, University of California, San Diego.

Gill, PE, Murray, W, and Saunders, MA (2002). SNOPT: An SQP algorithm for large-scale constrained optimization. SIAM Journal on Optimization;12(4):979-1006.

Gu Q. (2008). Finite element response sensitivity and reliability analysis of soil-foundation-structure-interaction (SFSI) systems, Doctor of Philosophy. University of California, San Diego, CA.

Huang, M. J., & Shakal, A. F. (1995). CSMIP strong-motion instrumentation and records from the I10/215 interchange bridge near San Bernardino. Earthquake spectra, 11(2), 193-215.

Lam, I. P., and Martin, G. R. (1986). "Sesimic Design of Highway Bridge Foundations." Federal Highway Administration, Washington D.C.

Malhotra, P. K., Huang, M. J., & Shakal, A. F. (1995). Seismic interaction at separation joints of an instrumented concrete bridge. Earthquake eng & structural dyn, 24(8), 1055-1067.

Storesund, R., Dengler, L., Mahin, S., Collins, B. D., Hanshaw, M., Turner, F., and Welsh, K. (2010). M6.5 Earthquake Offshore Northern California January 9, 2010. GEER Field Reconnaissance Summary.

Wang, N., Elgamal, A., & Lu, J. (2018). Assessment of the Samoa Channel Bridge-foundation seismic response. Soil Dynamics and Earthquake Engineering, 108, 150-159.

Wang, N., Elgamal, A., & Lu, J. (2020). Assessment of the Eureka Channel Bridge-foundation seismic response. (in preparation).

Zafir, Z. (2002). "Seismic Foundation Stiffness for Bridges." Proc., Deep Foundations 2002: An International Perspective on Theory, Design, Construction, and Performance, ASCE, GSP 116, Orlando, Florida, 1421-1437.

Zeghal, M. (1990). System identification of the nonlinear seismic response of earth dams, Ph.D. Thesis, Princeton University, Princeton, NJ.